UNIVERSITY OF PARDUBICE

FACULTY OF CHEMICAL TECHNOLOGY

Department of Biological and Biochemical Sciences

Pavlína Majtnerová

DEVELOPMENT OF A SPECTROFLUOROMETRIC METHOD FOR DETECTION OF NUCLEAR CONDENSATION AND FRAGMENTATION IN CELLS

Theses of the Doctoral Dissertation

Pardubice 2021

Study program: **Analytical chemistry**

Study field: **Analytical chemistry**

Author: **Mgr. Pavlína Majtnerová**

Supervisor: **doc. RNDr. Tomáš Roušar, PhD**

Year of the defence: **2021**

References

MAJTNEROVÁ, Pavlína. Development of a spectrofluorometric method for detection of nuclear condensation and fragmentation in cells. Pardubice, 2021. 132 pages. Dissertation thesis (PhD.). University of Pardubice, Faculty of Chemical Technology, Department of Biological and Biochemical Sciences. Supervisor: doc. RNDr. Tomáš Roušar, PhD.

Abstract

The dissertation focuses on a brief description of the process of apoptosis, then on an overview of methods used in the detection of DNA breaks and DNA fragmentation. Especially, here we described fluorescent Hoechst probes which can be used to detect nuclear condensation and fragmentation via fluorescence microscopy and flow cytometry.

As part of experimental work, we developed a spectrofluorometric method using the Hoechst 33258 probe for the detection of nuclear condensation and fragmentation in cells and subsequent evaluation. Using this method, we detected the effect of selected toxins on the process of nuclear condensation and fragmentation *in vitro*. We supplemented the obtained results with other methods designed to detect apoptosis, such as the detection of caspase activity and changes in protein expression, or the TUNEL and DNA ladder methods. In the final part of the work, we summarized, discussed and compared the measured results with the literature.

Abstrakt

Disertační práce se zaměřuje na krátký popis procesu apoptózy, dále potom na přehled metod, které se využívají při detekci DNA zlomů a DNA fragmentace. Jsou zde popsány zejména fluorescenční sondy Hoechst, které lze využít k detekci kondenzace a fragmentace jádra buněk pomocí fluorescenční mikroskopie a průtokové cytometrie.

V rámci experimentální práce jsme vyvinuli spektrofluorimetrickou metodu využívající sondu Hoechst 33258 pro detekci nukleární kondenzace a fragmentace v buňkách i s následným vyhodnocením. Pomocí této metody jsme detekovali vliv zvolených toxinů na proces nukleární kondenzace a fragmentace *in vitro*. Získané výsledky jsme doplnili dalšími metodami určenými k detekci apoptózy, jako jsou např. detekce aktivity kaspáz a změn proteinové exprese, nebo metody TUNEL a DNA žebřík. V závěrečné části práce jsme naměřené výsledky shrnuli, diskutovali a porovnali s literaturou.

Keywords

Apoptosis, nuclear condensation and fragmentation, Hoechst 33258, DNA fragmentation.

Klíčová slova

Apoptóza, nukleární kondenzace a fragmentace, Hoechst 33258, DNA fragmentace.

Table of Contents

1 Introduction

1.1 *Apoptosis*

Apoptosis is a complex process including various morphological and biochemical cellular changes that can be used for apoptosis characterization. The morphological changes include cell shrinkage, pyknosis and karyorrhexis followed by DNA fragmentation in late stage of apoptosis (Elmore, 2007; Wyllie, 1980). Then, the cellular cytoskeleton is damaged leading to membrane blebbing and, finally, apoptotic bodies formation (Elmore, 2007; Wyllie, 1980).

Pyknosis is an irreversible process of nuclear condensation commonly associated with early stages of apoptosis and necrosis (Hou et al., 2016). Pyknosis can be divided into nucleolytic and anucleolytic pyknosis (Burgoyne, 1999). Nucleolytic pyknosis mainly occurs during apoptosis. Chromatin is condensed into large clumps which can be packed into apoptotic bodies. In contrast, anucleolytic pyknosis predominantly occurs during necrosis when chromatin condenses into smaller, irregular clumps (Gotzmann et al., 2000; Hou et al., 2016).

Karyorrhexis occurs during late stage of apoptotic and necrotic processes when nucleus is fragmented and chromatin irregularly distributed into the cytoplasm, followed by formation of apoptotic bodies and karyolysis, respectively. Karyolysis is a complete enzymatic degradation of chromatin in dying cells (Takada et al., 2020). Nuclear condensation and fragmentation have been used as markers for late stages of apoptosis (Ferri and Kroemer, 2000).

Caspases play crucial roles in apoptosis. Caspases 8, 9 and 10 initiate apoptotic cascade through activation of efector caspases 3, 6 and 7 (Walsh et al., 2008). DNA fragmentation factor (DFF) has an essential role in DNA cleavage during the apoptotic process. Activated caspase 3 cleaves the DFF, and activates its catalytic subunit (DFF40) (Zhou et al., 2001). Activated DFF40 cleaves double-stranded DNA with a preference for adenine and thymine (A/T) rich region in internucleosomal linker regions into approx. 180 bp fragments and multiples thereof (Nagata et al., 2003; Wyllie, 1980). This characteristic DNA cleavage pattern is called “DNA ladder” and can be used for detection of apoptotic DNA fragmentation (Skalka et al., 1976; Wyllie, 1980). In addition to DNA ladder, comet and Terminal deoxynUcleotidyl transferase Nick-End Labeling (TUNEL) assays belong among frequently used methods for apoptotic DNA fragmentation detection. DNA ladder assay uses the presence of the DNA ladder fragments pattern occurring during apoptosis detected after electrophoresis in agarose gel, while comet detects fragmented DNA in the gel. In the TUNEL technique, free -OH moiety in the double and single strand DNA breaks is labeled using modified deoxynucleotides analogues tagged with various markers allowing DNA strand breaks detection (Majtnerová and Roušar, 2018).

1.2 *Apoptosis detection using Hoechst fluorescent probes*

Chromatin condensation and DNA fragmentation can be also characterized using microscopic methods, especially fluorescence microscopy. Hoechst fluorescent probes originate from bisbenzimides, a family of lipophilic substances, that bind preferentially

to a small groove of A/T rich DNA sequences called A-T regions (Martin et al., 2005). At least three consecutive A-T base pairs are required for specifc Hoechst dye binding leading to fluorescence increase. In addition, some papers reported that the nucleus of apoptotic cells can exhibit enhanced fluorescence after Hoechst binding (Zhang et al., 2007). Therefore, Hoechst probes have been frequently used for nucleus staining in fluorescence microscopy and flow cytometry (Gomes et al., 2018; Liu et al., 2017).

At present, three Hoechst probes have been used *in vitro*: 33258 (Vardevanyan et al., 2020), 33342 (Campos et al., 2018), 34580 (Nogueira et al., 2016). Hoechst 33258 is a lipophilic and cell permeable probe (Zhou et al., 2018) most frequently used in fluorescence microscopy for qualitative detection of nuclear morphology changes, primarily for detecting cell shrinkage, chromatin condensation, nuclear fragmentation and apoptotic bodies formation in various cell lines (Chen et al., 2012; Kapoor et al., 2013). Despite the unique Hoechst probe properties for nuclear changes detection, no scientific study, however, reported a quantitative spectrofluorometric method development. Thus, the aim of the present study was to develop a Hoechst 33258 (H33258) dye spectrofluorometric assay for quantitative measurement of nuclear condensation and fragmentation in intact cells. Finally, we aimed to evaluate the obtained outcomes in comparison with other frequently used methods for cell damage (i.e. WST-1 and glutathione assays) and apoptosis (TUNEL, DNA ladder, etc.) detection.

2 Experimental Part

2.1 *Aim of PhD study*

The main aim of the study was to develop a spectrofluorometric method for nuclear condensation and fragmentation detection in intact cells using fluorescent probe Hoechst 33258. Furthmore, our goal was to use apoptotic inducers (cisplatin, camptothecin, staurosporine) for nuclear condensation and fragmentation detection and to compare this method with other biochemical and biological methods.

2.2 *Cell culture and treatment*

All materials for cell culture were purchased from Sigma-Aldrich (USA) if not otherwise specified. HepG2 cells (ATCC HB-8065), a human hepatocellular carcinoma cell line, were purchased from ATCC (Manassas, VA, USA). HepG2 cells were cultured in Dulbecco's Modified Eagle's Medium with high glucose content (4500 g/L, w/wo phenol red) supplemented with 10% (v/v) fetal bovine serum, 50 μg/mL penicillin, 50 μg/mL streptomycin, 10 mM HEPES and 2 mM glutamine, maintained at 37°C in a sterile, humidified atmosphere of 5% CO_2. All the experiments were conducted using HepG2 cells in passages 4-15.

Human kidney, HK-2 cells (ATCC CRL-2190), a proximal tubular epithelial cell line derived from normal adult human kidney cells immortalized by transduction with human papillomavirus (HPV 16) DNA fragment (Ryan et al., 1994), were purchased from the ATCC (Manassas, VA, USA). The cells were cultured in supplemented

Dulbecco's modified Eagle's medium (DMEM/F12 = 1:1) with 5% (v/v) fetal bovine serum, 1 mM pyruvate, 10 μg/mL insulin, 5.5 μg/mL transferrin, 5 ng/mL sodium selenite, 50 μg/mL penicillin, 50 μg/mL streptomycin, and 5 ng/mL epidermal growth factor according to a published protocol (Handl et al., 2019; Hauschke et al., 2017). All the experiments were conducted using the HK-2 cells in passages 5-15.

HepG2 and HK-2 cells were tested for mycoplasma contamination using the MycoAlert Mycoplasma Detection Kit (Lonza). All cells used in the experiments were mycoplasma free. Short tandem repeat (STR) analysis (i.e., DNA fingerprinting) was used for HepG2 and HK-2 cell line authentication using a commercial kit in Generi Biotech (Czech Republic). The STR analysis proved 100% conformity of both HepG2 and HK-2 cells with the reference standards.

The HepG2 and HK-2 cells were seeded in 100 μL of appropriate cell culture medium in 96-well plates at density of $15x10^3$ and $20x10^3$ cells per well for 24 h (if not stated otherwise). To induce cell impairment, we used: cisplatin (CisPt, 0-100 μM), camptothecin (CAM; 0-5 μM), staurosporine (STA; 0-100 nM) and TiO_2 P25 nanoparticles (NPs; 0-10 μg/mL). All compounds were diluted in appropriate cell culture mediums to obtain final concentrations. After seeding, the culture medium was replaced by 100 μL of medium containing a tested compound and the cells were treated for 6, 24 and 48 h. To characterize the extent of cell impairment, we used the newly developed spectrofluorometric assay using H33258 together with caspase activity and proteins expression measurements, TUNEL and DNA ladder assays.

2.3 *Spectrofluorometric detection of nuclear condensation and fragmentation*

To develop a spectrofluorometric method for detection of changes in nuclear condensation and fragmentation in intact cells, we used a fluorescence dye H33258. To optimize the assay, we used HepG2 and HK-2 cells at confluency 50-70%. After treatment with tested compounds (CisPt, CAM, STA, NPs) for 6, 24 and 48 h, the cells grown in a 96-well plate were centrifuged (5 min, 8000*g*) at RT. Then, 70 μL of a supernatant was replaced with 70 μL of warmed phosphate-buffered saline (PBS 1x, 37 °C) and 10 μL of H33258 solution (in PBS 1x) was added to a well. The final concentrations of H33258 in a well were 0.1-5 μg/mL. Then, the cells were incubated with H33258 for 60 minutes during optimization of the assay, or for 5 min at optimal conditions and the spectrofluorometric measurement was performed at EX/EM=352/461 nm (EX/EM slit widths 25/25 nm) using a Tecan Spark fluorescence microplate reader (Tecan, Austria) while incubated at 37 °C. The samples were measured at least in triplicates. After background subtraction, the fluorescence signal was presented in Relative Fluorescence Units (RFU) as mean ± SEM. All spectrofluorometric measurements presented here were repeated at least in three independent experiments.

2.4 *WST-1 assay*

Dehydrogenase activity was evaluated by WST-1 test (Roche, Germany). The WST-1 test measures the activity of intra- and extramitochondrial dehydrogenases. After cell treatment, 10 μL of WST-1 reagent was added to the treated cells. The

absorbance change (0–1 h) was measured spectrophotometrically at wavelength of 440 nm using a Tecan Spark fluorescence microplate reader (Tecan, Austria). The cell viability was expressed as the percentage of intra- and extramitochondrial dehydrogenases activity relative to that in control cells (= 100%). The results were expressed as mean ± SD.

2.5 *Glutathione assay*

Glutathione levels were measured using the monochlorobimane spectrofluorometric assay (Capek et al., 2017). After cell treatment, 20 µL of the bimane solution was added to cells to obtain the final concentration 40 µM and spectrofluorometric measurement was started immediately. The fluorescence increase (EX/EM=394/490 nm) was measured for 10 min using a Tecan Spark fluorescence microplate reader (Tecan, Austria). The fluorescence was expressed as the slope of change in fluorescence over time. The glutathione levels were expressed as the percentage relative to the glutathione levels in control cells (= 100%). The results were expressed as mean ± SD.

2.6 *Caspase activity detection*

Caspase 3/7 activity in HepG2 and HK-2 cells was detected using ApoONE Homogeneous Caspase-3/7 Assay (Promega, USA) according to the manufacturer´s instructions. Briefly, 100 µL of the caspase 3/7 working solution was added to treated cells. After mixing, the cells were incubated for 30 min. Then, the fluorescence (EX/EM=485/535 nm) was measured in duplicates using a Tecan Spark fluorescence microplate reader (Tecan, Austria) while incubated at 37 °C. The caspase 3/7 activity levels were expressed as the percentage relative to the caspase 3/7 activity levels in control cells (= 100%). The results were expressed as mean ± SEM.

2.7 *Capillary Western Immunoassay*

Capillary Western Immunoassay was performed in protein lysates from HepG2 and HK-2 cells cultured in 6-well plates at density of $5x10^5$ and $1.3x10^6$ cells per well, respectively. After seeding, the culture medium was replaced by 2 mL of CisPt solution and the cells were treated for 6, 24 and 48 h. After treatment, the cells were washed twice with PBS 1x and protein lysates were prepared by lysing cells with 400 µL of RIPA buffer (Sigma-Aldrich, USA) with MS-safe protease and phosphatase inhibitor (Sigma-Aldrich, USA) on ice. Capillary Western Immunoassay was performed according to manufacturer´s instructions (Protein Simple, USA). Briefly, protein lysates were analyzed on a Wes system (ProteinSimple, USA) using a 12–230 kDa Separation Module (Biotechne, UK). Levels of phosphorylated JNK (pJNK, primary antibody 1:50, Promega, USA), poly-(ADP-ribose) polymerase-1 (PARP-1; primary antibody 1:100; Cell Signalling, USA) were normalized using the reference protein β-actin (primary antibody 1:500, Sigma-Aldrich, USA). The peaks were analyzed using Compass software (Protein Simple, USA). Two criteria were used for the discrimination of signals from the background: 1) the peak high must be higher or equal to 1000 and 2) the peak´s

signal-to-noise ratio given by the software must be higher or equal to 10. The results were counted as: $\frac{\text{area of the peak of interest}}{\text{area of the peak of β-actin}}$.

2.8 *TUNEL assay*

TUNEL assay followed by H33258 staining of nuclei was performed in HepG2 and HK-2 cells cultured in 200 µL of appropriate cell culture medium on cell culture chamber slides at density of $1.5x10^5$ and $2x10^5$ cells per well, respectively. After seeding, the culture medium was replaced by 200 µL of CisPt solutions and the cells were treated for 6, 24 and 48 h. TUNEL assay was performed using Click-iT™ TUNEL Alexa Fluor™ 488 Imaging Assay kit (ThermoFisher Scientific, USA) according to manufacturer´s instructions. The cells were fixed with 12% formaldehyde for 15 min at 37 °C. Then, the cells were permeabilized with 0.2% Triton X-100 for 15 min at 37 °C, washed with PBS 1x and incubated with terminal deoxynucleotidyl transferase (TdT) buffer for 10 min at 37 °C. After incubation, cells were mixed with a TdT reaction mixture (TdT buffer, 5-Ethynyl-2'-deoxyuridine 5'-triphosphate, TdT) and incubated for 1 h at 37 °C. Then, the cells were washed with 3% bovine serum albumin (BSA) and Click IT reagent for fluorescent staining was added for 30 min at 37 °C. After PBS 1x washing, H33258 at a final concentration of 2 µg/mL was used to visualize the cell nuclei. DNA strand breaks (FITC filter, 480/30 nm) and cell nuclei (DAPI filter, 375/28 nm) were visualized with an Eclipse 80i fluorescence microscope (Nikon, Japan).

2.9 *DNA ladder assay*

DNA ladder assay was performed in HepG2 and HK-2 cells cultured in 6-well plates at density of $5x10^5$ and $1x10^6$ cells per well, respectively. After seeding, the culture medium was replaced by 2 mL of CisPt and the cells were treated for 6, 24 and 48 h. DNA was isolated from treated cells using The ApoTarget™ Quick Apoptotic DNA Ladder Detection Kit (Invitrogen, USA). Isolated DNA samples were loaded onto a 1.5% agarose gel with 0.5 mg/mL ethidium bromide (Top-Bio, Czech Republic) followed by electrophoresis (5 V/cm). Finally, DNA was visualized by an ultraviolet gel documentation system (Vilber Lourmat, Germany) at wavelength 254 nm. GeneRuler 100 bp DNA ladder (ThermoFisher Scientific, USA) was used as a DNA size standard.

2.10 *Statistical analysis*

Statistical analysis was performed using OriginPro 9.0.0 (OriginLab, USA). Statistical significance was analyzed after normality testing using one-way analysis of variance (ANOVA) followed by Tukey's test at significance level $p=0.05$ (*, $p<0.05$; **, $p<0.01$; ***, $p<0.001$).

3 Results

3.1 *Optimization of the spectrofluorometric assay*

We aimed to develop a spectrofluorometric method for detection of nuclear condensation and fragmentation in the intact cells using a fluorescent probe Hoechst 33258. According to the literature, we used the same $\lambda_{(ex,max)}$=352 nm and $\lambda_{(em,max)}$=461 nm in H33258 measurements (Hadi et al., 2018), but optimized the experimental procedure, i.e. H33258 concentration and incubation length of the probe with cells. To induce cell damage, we incubated HepG2 cells with 100 μM CisPt for 24 h. Then, we incubated the cells with the concentrations range of 0.1-5 μg/mL H33258 (Fig. 1). The highest fluorescence signal was detected in 5 μg/mL H33258 in CisPt treated cells but the background fluorescence in untreated HepG2 cells was strongly enhanced too. Due to the highest signal-to-noise ratio found after the 2 μg/mL, we selected this H33258 treatment concentration to be optimal for following experiments.

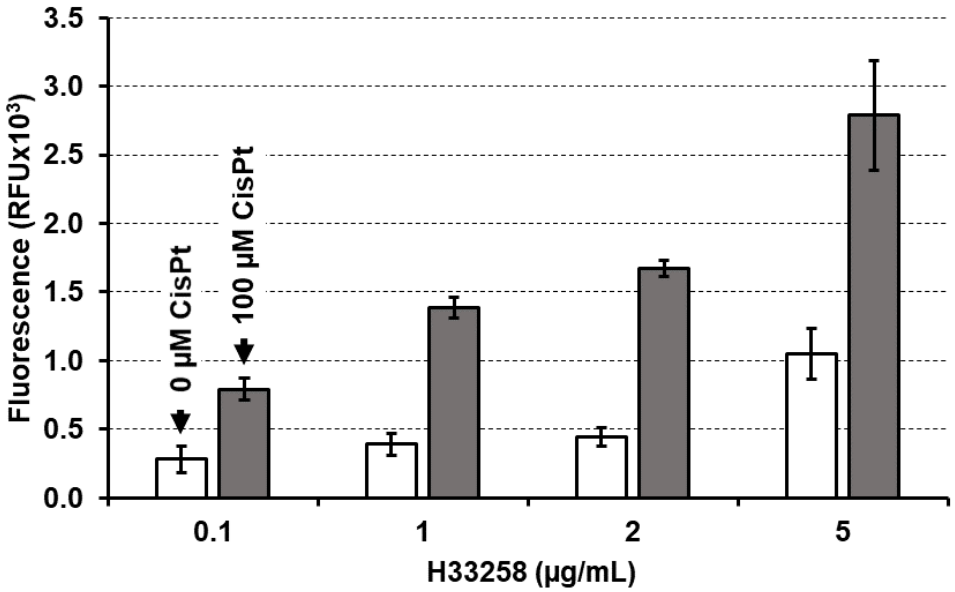

Figure 1: Optimization of H33258 concentration (HepG2 cells). H33258 concentrations 0.1; 1; 2; 5 μg/mL. Cisplatin (CisPt; 0-100 μM). 0 μM CisPt (white columns), 100 μM CisPt treated cells (grey columns). Mean ± SEM (n=3).

For estimation of optimal cell incubation time with H33258, HepG2 cells were treated with CisPt (0; 50; 100 μM) for 24 h. We found that centrifugation of cells (5 min, 8000*g*; RT) after the treatment with tested compounds, followed by cell culture medium replacement, is crucial for achieving repeatable results because it ensures the sedimentation of all cells on the bottom of a well. After centrifugation, 70 μL of culture medium was replaced with 70 μL of PBS 1x in each well. Then, 10 μL of H33258 was added to obtain final concentration 2 μg/mL H33258 in a well and fluorescence was recorded at EX/EM=352/461 nm. We found that fluorescence intensity was increasing strongly during the first minute of cells incubation with H33258 (Fig. 2).

Then, the fluorescence intensity (IF) remained rather stable between the second and the tenth minute of incubation implying that any of durations including this time interval could be used for the purposes of the spectrofluorometric assay. We selected 5 min of

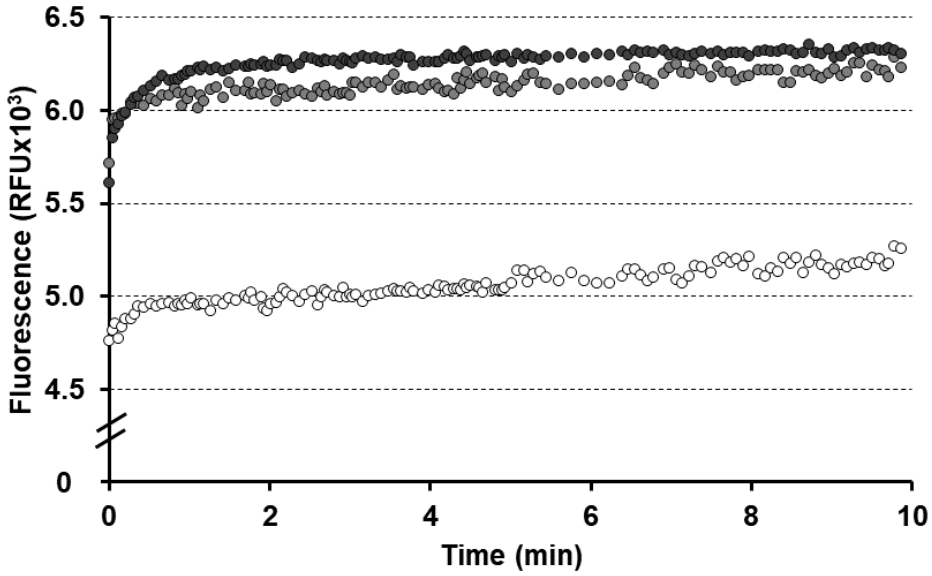

Figure 2: Change of intensity of fluorescence over time (HepG2 cells). Incubation with cisplatin for 24 h. Then, the cells were incubated with H33258 (2 µg/mL) and fluorescence (EX/EM=352/461 nm) was recorded for 10 min. Untreated cells (black), 50 µM CisPt (light grey), 100 µM CisPt (dark grey).

H33258 incubation with cells in all following experiments. In addition, we confirmed that IF was enhanced relatively to the increasing CisPt concentration in cells according to expected induction of nuclear condensation and fragmentation. Figure 3A shows IF detected in cells after subtraction of background fluorescence intensity in blank samples (i.e. without cells). Finally, the extent of nuclear condensation and fragmentation in cells was expressed in Relative Fluorescence Units (RFU) (Fig. 3B)

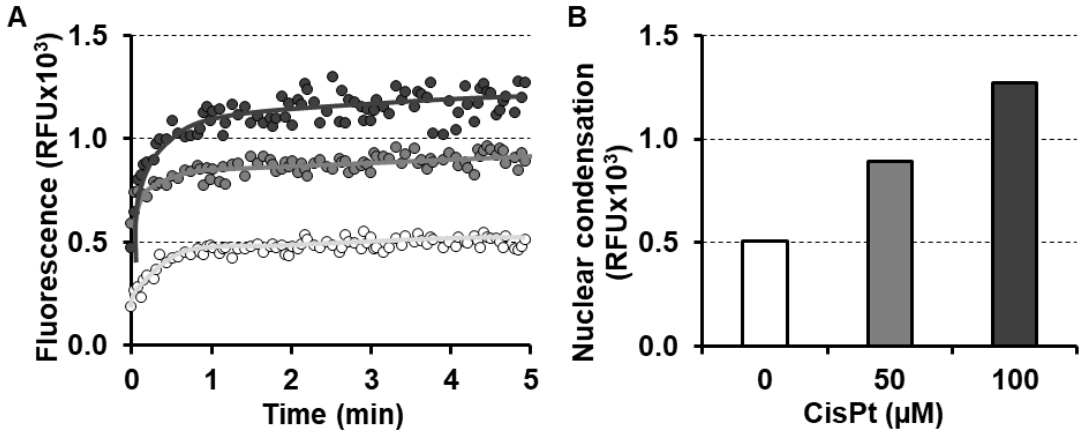

Figure 3: Detection of nuclear condensation and fragmentation in cells. HepG2 cells were treated with cisplatin for 24 h. Then, the cells were incubated with H33258 (2 µg/mL) and fluorescence (EX/EM=352/461 nm) was recorded for 5 min. Finally, the background fluorescence was subtracted and fluorescence intensity corresponding to the extent of nuclear condensation and fragmentation was showed in untreated (white), 50 µM (light grey) and 100 µM CisPt (dark grey) treated cells (=A). The fluorescence intensity attributed to the extent of nuclear condensation and fragmentation was compared among untreated cells (white), 50 µM CisPt (light grey), 100 µM CisPt (dark grey) treated cells (=B).

3.2 *Estimating sensitivity of the spectrofluorometric assay*

Further aim of our study was to use the H33258 spectrofluorometric assay in cells exhibiting nuclear condensation and fragmentation of different origin and extent. We incubated HepG2 and HK-2 cells with CisPt (0; 0.5; 5; 25 and 100 μM) for 24 and 48 h. After H33258 treatment, we observed increasing IF relating to both CisPt doses and incubation time in HepG2 (Fig. 4) and HK-2 cells (Fig. 5). We found a significant increase of IF in 25 and 100 μM CisPt treated cells afer 24 and 48 h. In addition, the extent of nuclear condensation and fragmentation detected after 24 and 48 h demonstrated time and dose dependent increase (Fig. 4 and 5).

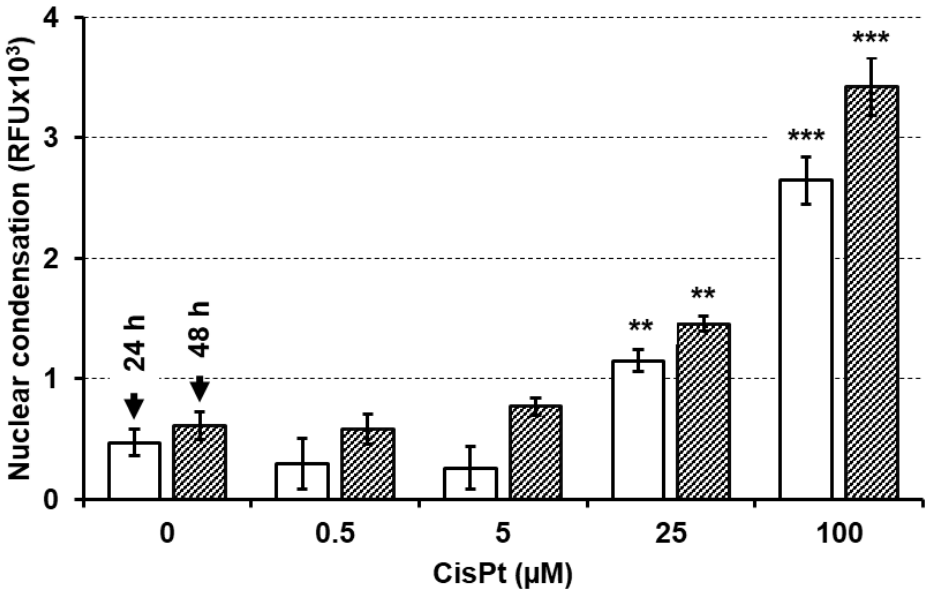

Figure 4: Detection of nuclear condensation and fragmentation (HepG2 cells). Cisplatin (CisPt; 0; 0.5; 5; 25 and 100 μM). Incubation 24 and 48 h. Fluorescence intensity (EX/EM=352/461 nm). Mean ± SEM (**, *p<0,01;* ***, *p<0.001*, vs. untreated cells at appropriate time interval).

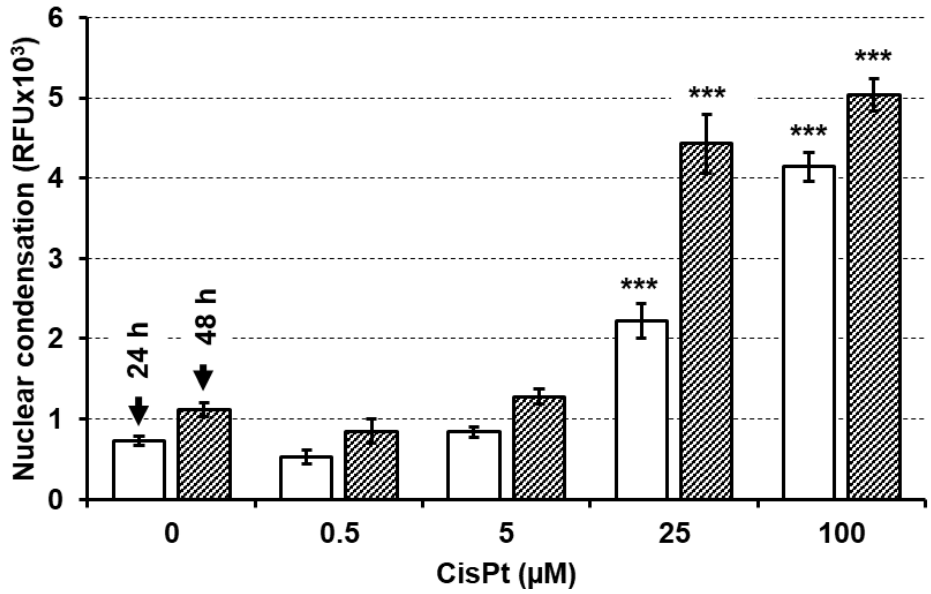

Figure 5: Detection of nuclear condensation and fragmentation (HK-2 cells). Cisplatin (CisPt; 0; 0.5; 5; 25, 100 μM). Incubation 24 and 48 h. Fluorescence intensity (EX/EM=352/461 nm). Mean ± SEM (***, *p<0.001*, vs. untreated cells at appropriate time interval).

We used two additional biochemical assays to estimate sensitivity of spectrofluorometric H33258 assay, i.e. the WST-1 test detecting intracellular dehydrogenase activity and glutathione assay. We found considerably reduced dehydrogenase activity in HepG2 treated with ≥25 μM CisPt (Fig. 6) and for all CisPt treatment of HK-2 cells in 24 h treatment (Fig. 7), while for both cells type in 48 h treatment, the doses ≥5 μM CisPt had significant reduction.

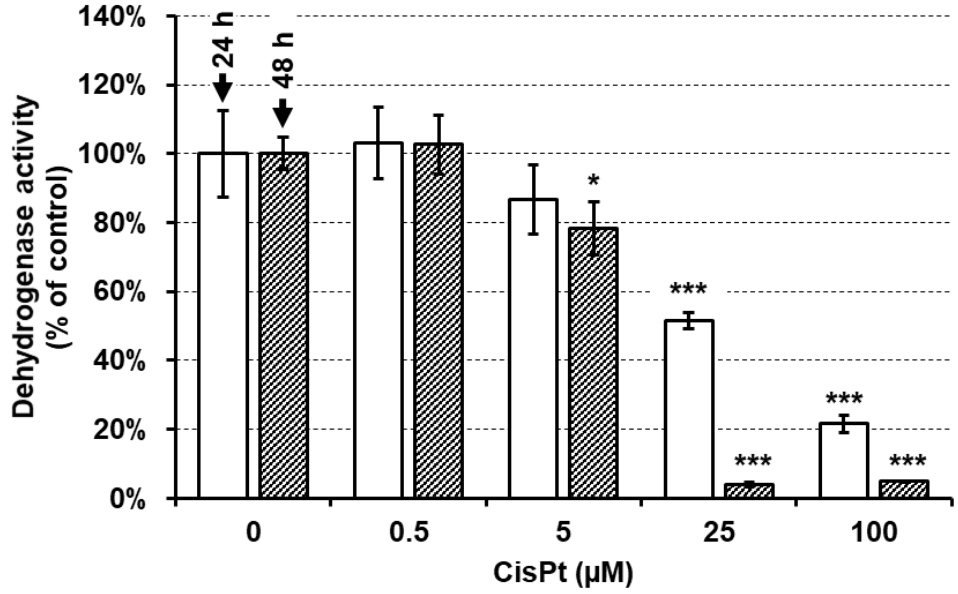

Figure 6: Dehydrogenase activity using the WST-1 test (HepG2 cells). Cisplatin (CisPt; 0; 0.5; 5; 25 and 100 M). Incubation 24 and 48 h. Absorbance (440 nm). Mean ± SD (*, *p<0.05;* ***, *p<0.001*, vs. untreated cells at appropriate time interval).

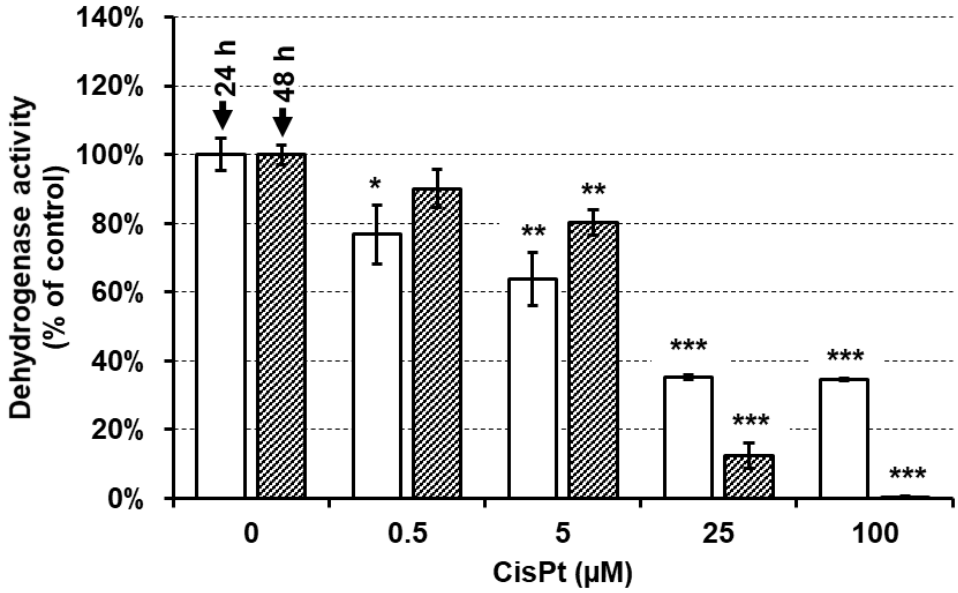

Figure 7: Dehydrogenase activity using the WST-1 test (HK-2 cells). Cisplatin (CisPt; 0; 0.5; 5; 25 and 100 μM). Incubation 24 and 48 h. Absorbance (440 nm). Mean ± SD (*, *p<0.05*; **, *p<0,01;* ***, *p<0.001* vs. untreated cells at appropriate time interval).

On the other hand, the HK-2 cell line exhibited lower susceptibility to glutathione depletion than HepG2 cells because a significant reduction of glutathione levels was found only at 100 μM CisPt (Figs. 8, 9) for 24 h treatment, while for HepG2 the significant reduction was ≥25 μM. For 48 h treatment, both cell types had significant reduction in similar CisPt concentrations treatments ≥5 μM.

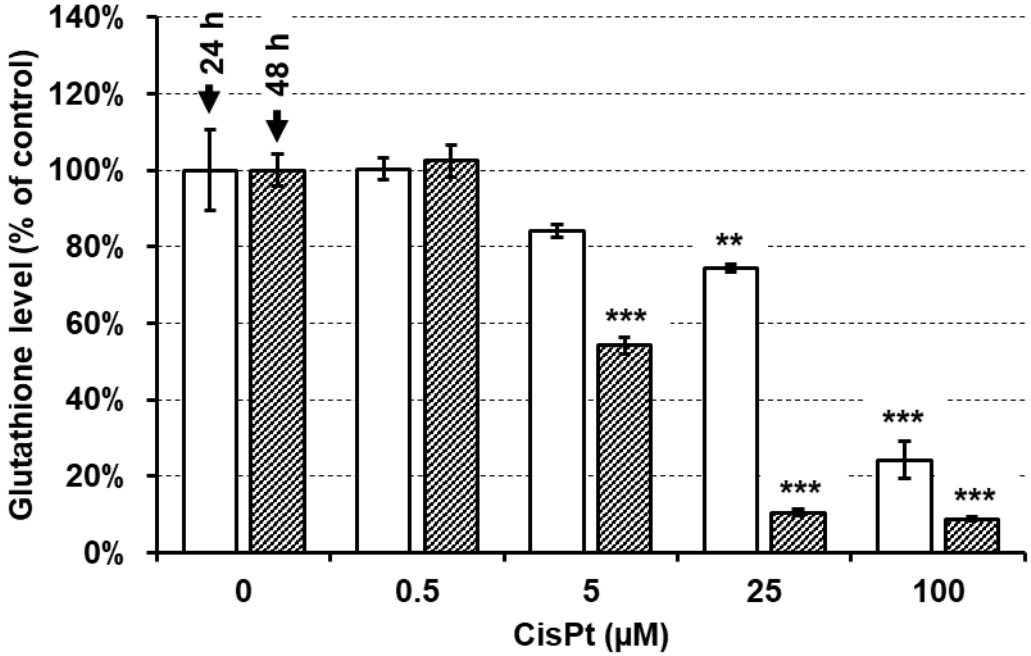

Figure 8: Glutathione level using the monochlorobimane assay (HepG2 cells). Cisplatin (CisPt; 0; 0.5; 5; 25 and 100 μM). Incubation 24 and 48 h. Fluorescence intensity (EX/EM=394/490 nm). Mean ± SD (**, *p<0,01;* ***, *p<0.001*, vs. untreated cells at appropriate time interval).

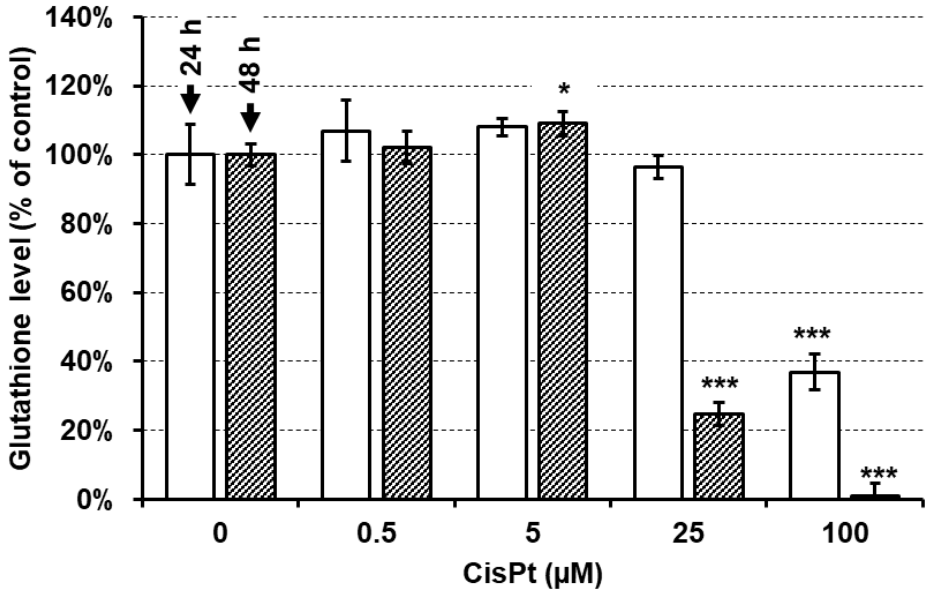

Figure 9: Glutathione level using the monochlorobimane assay (HK-2 cells). Cisplatin (CisPt; 0; 0.5; 5; 25 and 100 μM). Incubation 24 and 48 h. Fluorescence intensity (EX/EM=394/490 nm). Mean ± SD (*, *p<0.05;* ***, *p<0.001*, vs. untreated cells at appropriate time interval).

In conclusion, the outcomes found using the WST-1 and glutathione assays confirmed the occurrence of CisPt toxicity detected using the H33258 spectrofluorometric assay. WST-1 and glutathione assays detected cellular damage also in cells treated with 5 μM CisPt. Hence, both biochemical assays are more sensitive in detection of a cell damage in comparison to H33258 assay detecting structural nuclear changes. In addition to CisPt, we aimed to utilize the spectrofluorometric assay for detection of nuclear changes in cells treated with other apoptotic inducers. Thus, we incubated HepG2 and HK-2 cells with camptothecin (CAM, 1; 5 μM) and staurosporine (STA, 10; 100 nM) for 6, 24 and 48 h (Figs. 10 and 11).

We used CisPt as a positive control and 10 μg/mL TiO_2 P25 nanoparticles as a negative control. All results were compared to the signal in untreated cells at appropriate time interval. Our results showed that we detected a significant increase of nuclear condensation and fragmentation in all tested compounds except of TiO_2 P25 nanoparticles which did not induce any detected nuclear changes at all tested time durations.

After 6 h of treatment, we found a significant increase of IF related to enhanced nuclear changes only in HK-2 cells treated with 5 μM CAM ($p<0.001$). At 24 h, a significant increase of nuclear condensation and fragmentation comparing with untreated cells was detected in all HK-2 treated cells with exception of 1 μM CAM ($p=0.198$) and 10 nM STA ($p=0.999$). We also found a significant increase of IF in HepG2 cells treated with higher concentrations of used apoptotic inducers. Thus, the H33258 assay did not detect a significant nuclear condensation and fragmentation in 1 μM CAM ($p=0.935$), 10 nM STA ($p=0.135$) and 50 μM CisPt ($p=0.382$) treated HepG2 cells for 24 h.

After 48 h of treatment, we found significantly increased extent of nuclear condensation and fragmentation in almost all tested concentrations of compounds in both cell lines. The only exception was observed in 10 nM STA treated HepG2 cells ($p=0.999$) which exhibited a decrease of IF in comparison with 10 nM STA treated cells for 24 h. All tested concentrations of pro-apoptotic compounds induced larger nuclear condensation after 48 h incubation in comparison to 24 h and the cells treated with higher concentrations of tested compounds exhibited larger nuclear impairment in comparison to lower dose. The highest IF signal was detected in HepG2 and HK-2 cells treated with 100 μM CisPt and 5 μM CAM at 48 h. In conclusion, our results confirmed that the H33258 spectrofluorometric assay was capable to detect increased nuclear condensation and fragmentation in all tested apoptotic inducers relatively to concentration and incubation period (Figs. 10 and 11).

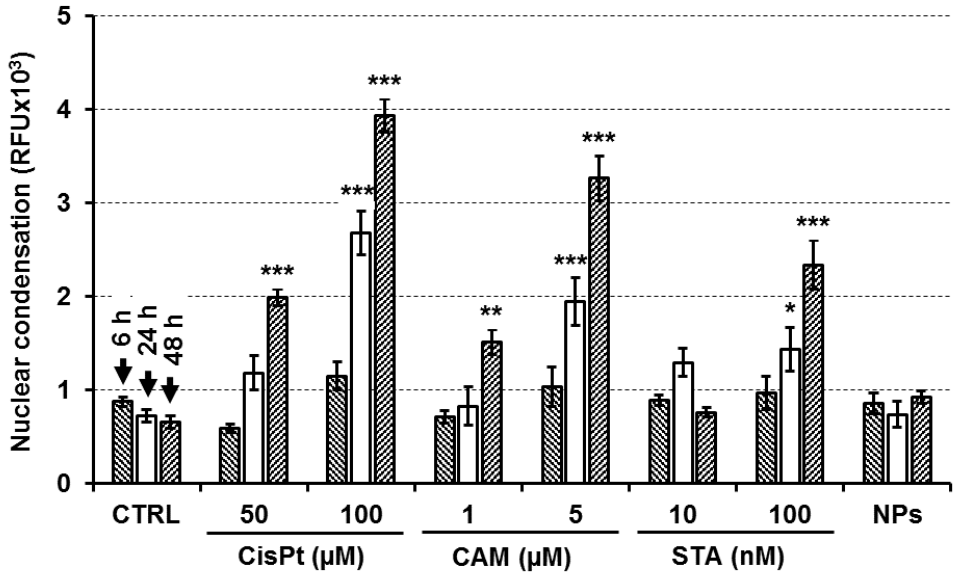

Figure 10: Detection of nuclear condensation and fragmentation using H33258 assay (HepG2 cells). Control cells (CTRL), cisplatin (CisPt; 0-100 μM), camptothecin (CAM; 0-5 μM), staurosporine (STA; 0-100 nM), TiO_2 nanoparticles P25 (NPs; 10 μg/mL). Incubation 6, 24 and 48 h. Flluorescence intensity (EX/EM=352/461 nm) in 5 min. Mean ± SEM (n=4); (**, p<0,05; **, p<0,01; ***, p<0,001,* vs. untreated cells at appropriate time interval).

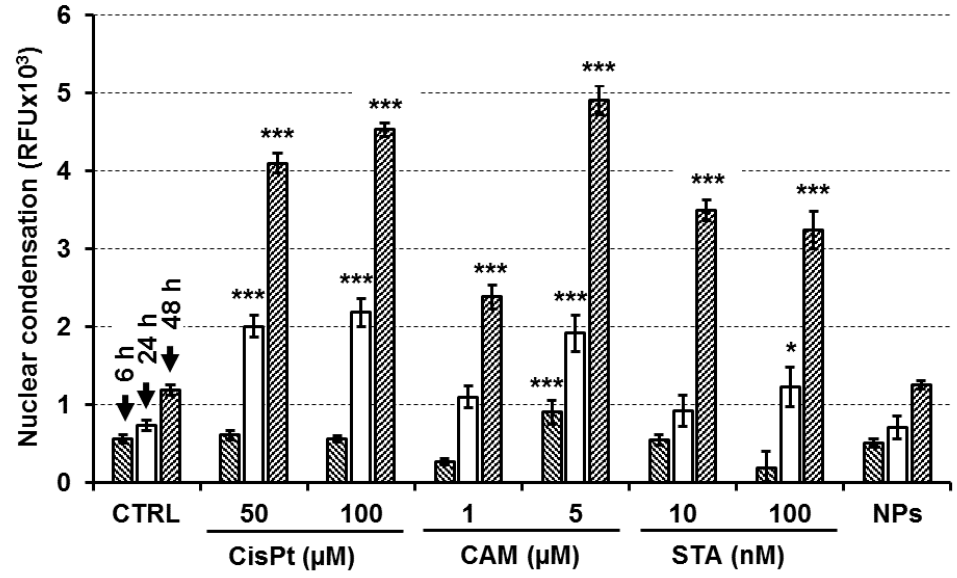

Figure 11: Detection of nuclear condensation and fragmentation using H33258 assay (HK-2 cells. Control cells (CTRL), cisplatin (CisPt; 0-100 μM), camptothecin (CAM; 0-5 μM), staurosporine (STA; 0-100 nM), TiO_2 nanoparticles P25 (NPs; 10 μg/mL). Incubation 6, 24 and 48 h. Fluorescence intensity (EX/EM=352/461 nm) in 5 min. Mean ± SEM (n=4); (**, p<0,05; **, p<0,01; ***, p<0,001,* vs. untreated cells at appropriate time interval).

3.3 *Comparison of H33258 assay with apoptosis detecting methods*

To evaluate the outcomes of newly developed H33258 spectrofluorometric assay, we aimed to compare the results with other methods characterizing pro-apoptotic

processes in cells. Therefore, we treated HepG2 and HK-2 cells with CisPt (50 and 100 μM) for 6, 24 and 48 h and characterized nuclear changes and pro-apoptotic activation using four additional measurements, i.e. caspase 3/7 activity, PARP-1 and JNK proteins expression, TUNEL assay and DNA ladder.

We measured the activity of caspases 3 and 7 to evaluate apoptotic activation in the cells. Despite detecting a significant increase in caspase 3/7 activity in both cell lines treated with 100 μM CisPt for 6 h, the largest enhancement of caspase 3/7 activity was detected in cells treated with 50 μM CisPt for 24 h (Figs. 12 and 13). At 48 h, the caspase 3/7 activities remained increased although we found a decrease in comparison to cells treated for 24 h.

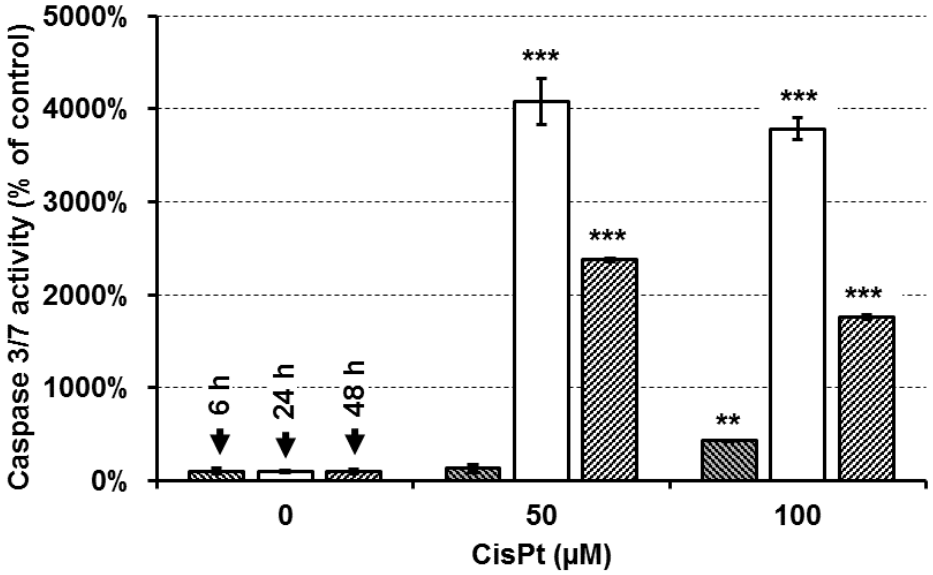

Figure 12: Caspase 3/7 activity (HepG2 cells). Cisplatin (CisPt; 0-100 μM). Incubation 6, 24 and 48 h. Fluorescence intensity (EX/EM=485/535). Mean ± SD (n=2); (**, *p<0,01;* ***, *p<0,001,* vs. untreated cells at appropriate time interval).

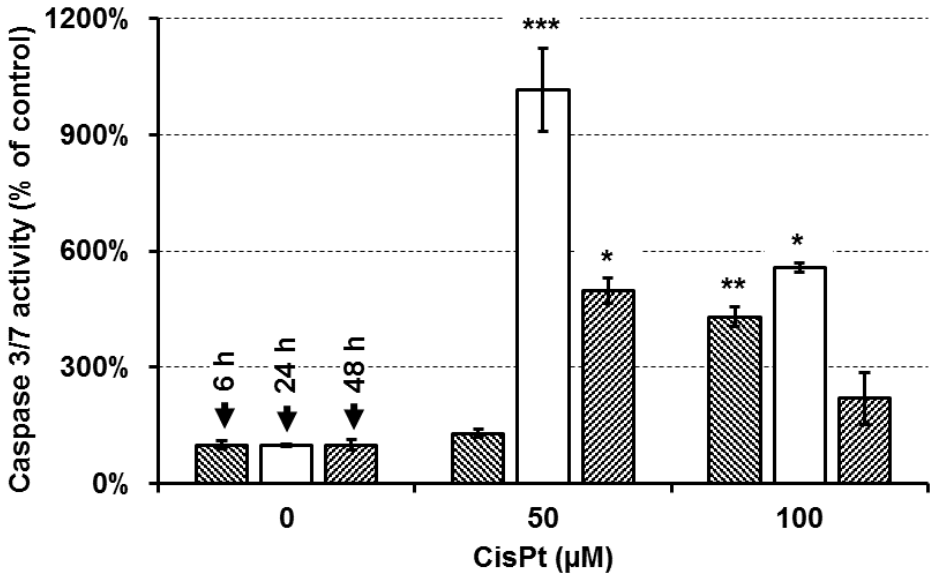

Figure 13: Caspase 3/7 activity (HK-2 cells). Cisplatin (CisPt; 0-100 μM). Incubation 6, 24 and 48 h. Fluorescence intensity (EX/EM=485/535). Mean ± SD (n=2); (*, *p<0,05;* **, *p<0,01;* ***, *p<0,001,* vs. untreated cells at appropriate time interval).

Then, we analyzed the levels of PARP-1, PARP-1 fragment (fPARP-1), pJNK and β-actin. PARP-1 protein serves as a substrate for caspase 3 during apoptosis. Thus, PARP-1 cleavage leading to fPARP-1 production is related to the extent of caspase 3 activation. Afer 24 h of treatment, we detected PARP-1 fragmentation in cells treated with both concentrations of CisPt which persisted until 48 h only in HepG2 cells (Table 1). Phosphorylation of JNK1 and JNK2 can also correspond with activated apoptotic process and that is why we aimed to estimate their levels. We observed that pJNK1 levels were increased in all tested time incubation with CisPt in HepG2 cells. In HK-2 cells, protein expressions of pJNK1 and pJNK2 were stimulated predominantly at 24 h of treatment. Thus, the detected increase of pJNK levels correlated strongly with PARP-1 fragmentation in both cell lines.

Table 1: PARP and JNK protein expressions in CisPt treated cells. HepG2 and HK-2 cells were treated with CisPt (50 and 100 μM) for 6, 24 and 48 h. After incubation, the protein expression of PARP-1, fPARP-1, pJNK1 and pJNK2 was analyzed using *Simple Western*. The results were expressed as a ratio: $\frac{\text{area of the peak of interest}}{\text{area of the peak of } \beta-\text{actin}}$.

		HepG2				HK-2			
Time	**CisPt (μM)**	**PARP-1**	**fPARP-1**	**pJNK1**	**pJNK2**	**PARP-1**	**fPARP-1**	**pJNK1**	**pJNK2**
6 h	0	2.3	0	0	0	0.4	0.1	0	0
	50	2.3	0	0.2	0.2	0.9	0.1	0	0
	100	1.8	0	0.4	0.3	0.7	0.5	0.1	0.1
24 h	0	1.9	0	0	0	1.6	0.1	0.1	0
	50	1.9	1.3	0.2	0.2	0.9	1.5	0.2	0.1
	100	2.7	2.0	0.7	0.6	0.8	1.5	0.3	0.2
48 h	0	3.0	0	0	0	0.9	0	0	0
	50	3.2	1.3	0.5	0	0.9	0.1	0	0
	100	3.2	1.0	1.2	1.0	0	0	0	0

TUNEL assay was used for detection of DNA strand breaks in CisPt treated cells (Fig. 14). Afer 6 h of treatment, a weak fluorescence demonstrating presence of DNA strand breaks was observed only in 100 μM CisPt treated HepG2 cells. At longer time durations, TUNEL staining detected strong DNA fragmentation in both cell lines treated with both 50 and 100 μM CisPt.

At final, we used DNA ladder assay in CisPt treated cells to estimate the extent of DNA fragmentation. The internucleosomal DNA fragmentation can occur as the terminal feature of apoptosis. Thus, we detected DNA ladder pattern only in CisPt treated HepG2 cells afer 48 h (Fig. 15A) and in HK-2 cells after 24 and 48 h (Fig. 15B).

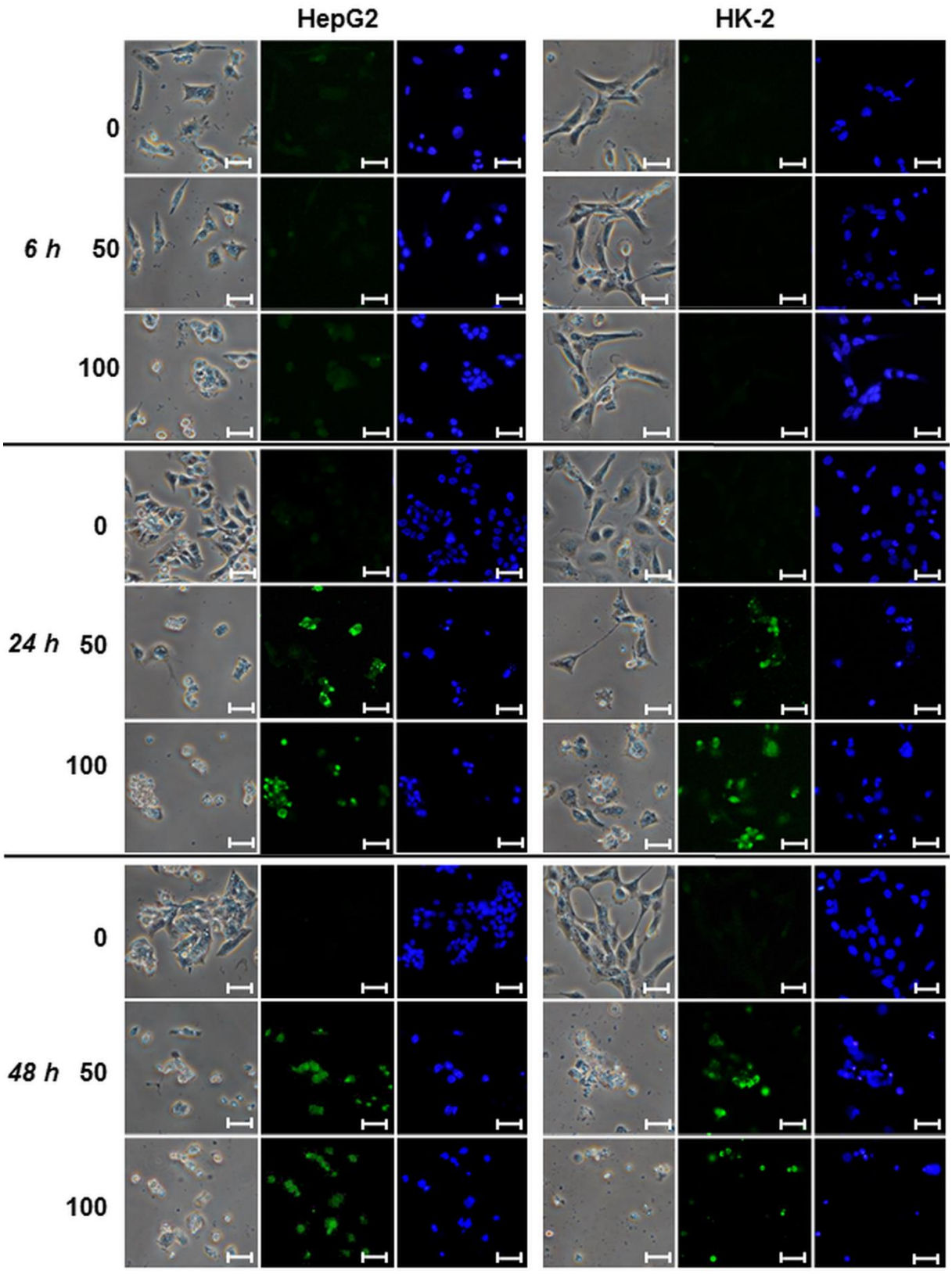

Figure 14: TUNEL assay in cisplatin treated cells. Cisplatin (CisPt; 0 – 0 μM; 50 – 50 μM; 100 – 100 μM). Incubation 6, 24 and 48 h. Phase contrast (left, magnification 400 ×), TUNEL (FITC 480/30 nm; middle) and Hoechst 33258 stainings (DAPI 375/28 nm; right). Scales correspond to 25 μm.

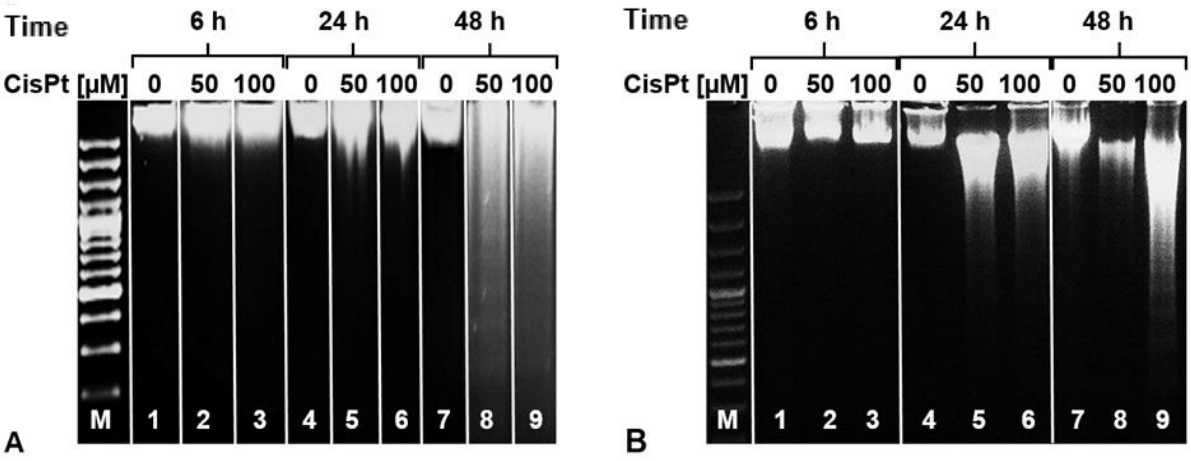

Figure 15: DNA ladder assay in cisplatin treated cells. A) HepG2 cells, B) HK-2 cells. Cisplatin (CisPt; 0, untreated cells; 50, 50 μM CisPt; 100, 100 μM CisPt; M, 100 bp marker). Incubation 6, 24 and 48 h.

We summarized and compared the results obtained using all methods detecting apoptosis in CisPt treated HepG2 and HK-2 cells (Table 2). We proved that the initial increase in caspase 3/7 activity was followed by fragmentation of PARP-1, DNA fragmentation detected using TUNEL assay and formation of DNA ladder. In addition, Table 2 shows that the newly developed spectrofluorometric assay using the H33258 dye provided outcomes fully comparable with TUNEL assay which has been used as a standard method detecting increased levels of DNA fragmentation in cells.

Table 2: Comparison of assays detecting pro-apoptotic changes. HepG2 and HK-2 cells were treated with 100 μM CisPt for 6, 24 and 48 h. After treatment, the nuclear changes were detected using five methods, i.e. developed spectrofluorometric assay using Hoechst 33258 (=H33258), caspase 3/7 activity, TUNEL assay, protein expression of PARP-1 fragment (fPARP-1) and DNA ladder. (−, negative;+/−, moderately positive;+, positive;++, strongly positive).

		H33258	***Caspases***	***TUNEL***	***fPARP-1***	***DNA ladder***
6 h	HepG2	+	+	+/-	-	-
	HK-2	-	++	-	+	-
24 h	HepG2	++	++	++	++	-
	HK-2	++	++	++	++	++
48 h	HepG2	++	++	++	++	++
	HK-2	++	-	++	-	++

4 Conclusion

We developed a spectrofluorometric method using Hoechst 33258 staining which detects nuclear condensation and fragmentation in intact cells. Our results showed that the spectrofluorometric method was capable to detect the nuclear changes in three typical pro-apoptotic agents, i.e. cisplatin, camptothecin, staurosporine, and in two cell lines of different origin.

In addition, we compared the results obtained using the spectrofluorometric assay with outcomes of other methods characterizing apoptotic processes. Based on this comparison, we conclude that here developed spectrofluorometric method is capable to detect nuclear pro-apoptotic changes of similar sensitivity and specificity to that of caspase 3/7 activity measurement and TUNEL assay. Therefore, we suppose that the spectrofluorometric H33258 method could join other routinely used methods characterizing apoptosis in cells. In comparison to TUNEL assay, the developed spectrofluorometric assay possesses several advantages (e.g. rapid processing, quantitative evaluation, low-cost) implying its potential use in assessing nuclear condensation and fragmentation in routine laboratory practice and in high-throughput screening studies.

5 List of references

Burgoyne, L.A. The mechanisms of pyknosis: Hypercondensation and death. *Exp Cell Res*. **1999** (248), 214-222.

Campos, V., Rappaz B., Kuttler F., Turcatti G., and Naveiras O. High-throughput, nonperturbing quantification of lipid droplets with digital holographic microscopy. *J Lipid Res*. **2018** (59), 1301-1310.

Capek, J., Hauschke M., Bruckova L., and Rousar T. Comparison of glutathione levels measured using optimized monochlorobimane assay with those from ortho-phthalaldehyde assay in intact cells. *J Pharmacol Tox Met*. **2017** (88), 40-45.

Elmore, S. Apoptosis: a review of programmed cell death. *Toxicol Pathol*. **2007** (35), 495-516.

Ferri, K.F., and Kroemer G. Control of apoptotic DNA degradation. *Nat Cell Biol*. **2000** (2), E63-64.

Gomes, C.J., Harman M.W., Centuori S.M., Wolgemuth C.W., and Martinez J.D. Measuring DNA content in live cells by fluorescence microscopy. *Cell Div*. **2018** (13), 6.

Gotzmann, J., Meissner M., and Gerner C. The fate of the nuclear matrix-associated-region-binding protein SATB1 during apoptosis. *Cell Death Differ*. **2000** (7), 425-438.

Hadi, L.M., Yaghini E., Stamati K., Loizidou M., and MacRobert A.J. Therapeutic enhancement of a cytotoxic agent using photochemical internalisation in 3D compressed collagen constructs of ovarian cancer. *Acta Biomater*. **2018** (81), 80-92.

Handl, J., Capek J., Majtnerova P., Petira F., Hauschke M., Rousarova E., and Rousar T. Transient increase in cellular dehydrogenase activity after cadmium treatment precedes enhanced production of reactive oxygen species in human proximal tubular kidney cells. *Physiol Res*. **2019** (68), 481-490.

Hauschke, M., Rousarova E., Flidr P., Capek J., Libra A., and Rousar T. Neutrophil gelatinase-associated lipocalin production negatively correlates with HK-2 cell impairment: Evaluation of NGAL as a marker of toxicity in HK-2 cells. *Toxicol In Vitro*. **2017** (39), 52-57.

Hou, L., Liu K., Li Y.H., Ma S., Ji X.M., and Liu L. Necrotic pyknosis is a morphologically and biochemically distinct event from apoptotic pyknosis. *J Cell Sci*. **2016** (129), 3084-3090.

Chen, G., Hu X., Zhang W., Xu N., Wang F.Q., Jia J., Zhang W.F., Sun Z.J., and Zhao Y.F. Mammalian target of rapamycin regulates isoliquiritigenin-induced autophagic and apoptotic cell death in adenoid cystic carcinoma cells. *Apoptosis*. **2012** (17), 90-101.

Kapoor, R., Rizvi F., and Kakkar P. Naringenin prevents high glucose-induced mitochondria-mediated apoptosis involving AIF, Endo-G and caspases. *Apoptosis*. **2013** (18), 9-27.

Liu, C.-H., Tsao M.-H., Sahoo S.L., and Wu W.-C. Magnetic nanoparticles with fluorescence and affinity for DNA sensing and nucleus staining. *RSC Advances*. **2017** (7), 5937-5947.

Majtnerová, P., and Roušar T. An overview of apoptosis assays detecting DNA fragmentation. *Molecular Biology Reports*. **2018** (45), 1469-1478.

Martin, R.M., Leonhardt H., and Cardoso M.C. DNA labeling in living cells. *Cytometry A*. **2005** (67), 45-52.

Nagata, S., Nagase H., Kawane K., Mukae N., and Fukuyama H. Degradation of chromosomal DNA during apoptosis. *Cell Death Differ*. **2003** (10), 108-116.

Nogueira, E., Cruz C.F., Loureiro A., Nogueira P., Freitas J., Moreira A., Carmo A.M., Gomes A.C., Preto A., and Cavaco-Paulo A. Assessment of liposome disruption to quantify drug delivery in vitro. *Biochim Biophys Acta*. **2016** (1858), 163-167.

Ryan, M.J., Johnson G., Kirk J., Fuerstenberg S.M., Zager R.A., and Torok-Storb B. HK-2: an immortalized proximal tubule epithelial cell line from normal adult human kidney. *Kidney Int*. **1994** (45), 48-57.

Skalka, M., Matyasova J., and Cejkova M. Dna in chromatin of irradiated lymphoid tissues degrades in vivo into regular fragments. *FEBS Lett*. **1976** (72), 271-274.

Takada, S., Watanabe T., and Mizuta R. DNase gamma-dependent DNA fragmentation causes karyolysis in necrotic hepatocyte. *J Vet Med Sci*. **2020** (82), 23-26.

Vardevanyan, P.O., Parsadanyan M.A., Antonyan A.P., Shahinyan M.A., and Karapetyan A.T. Spectroscopic study of interaction of various GC-content DNA with Hoechst 33258 depending on Na(+) concentration. *J Biomol Struct Dyn*. **2020** 1-5.

Walsh, J.G., Cullen S.P., Sheridan C., Luthi A.U., Gerner C., and Martin S.J. Executioner caspase-3 and caspase-7 are functionally distinct proteases. *P Natl Acad Sci USA*. **2008** (105), 12815-12819.

Wyllie, A.H. Glucocorticoid-induced thymocyte apoptosis is associated with endogenous endonuclease activation. *Nature*. **1980** (284), 555-556.

Zhang, X.T., Song T.B., Du B.L., Li D.M., and Li X.M. Caspase-3 antisense oligodeoxynucleotides inhibit apoptosis in gamma-irradiated human leukemia HL-60 cells. *Apoptosis*. **2007** (12), 743-751.

Zhou, P., Lugovskoy A.A., McCarty J.S., Li P., and Wagner G. Solution structure of DFF40 and DFF45 N-terminal domain complex and mutual chaperone activity of DFF40 and DFF45. *Proc Natl Acad Sci U S A*. **2001** (98), 6051-6055.

Zhou, Y.B., Liu H.X., Zhao N., Wang Z.M., Michael M.Z., Xie N., Tang B.Z., and Tang Y.H. Multiplexed imaging detection of live cell intracellular changes in early apoptosis with aggregation-induced emission fluorogens. *Sci China Chem*. **2018** (61), 892-897.

6 List of Student´s Published Works

Publications associated with the Ph.D. thesis topic in the journals with IF

Majtnerová P., Čapek J., Petira F., Handl J., Roušar T. Quantitative Spectrofluorometric Assay Detecting Nuclear Condensation and Fragmentation in Intact Cells. *Scientific Reports,* 2021, 11 (11921). *ISSN 2045-2322, https://doi.org/10.1038/s41598-021-91380-3*. ***(IF = 3,99)***

Majtnerová P. a Roušar T. An overview of apoptosis assays detecting DNA fragmentation. Molecular Biology Reports, 2018, 1-10. *ISSN 1573-4978, https://doi.org/10.1007/s11033-018-4258-9. (**IF = 1,889**)*

Other publications in the journals with IF

Handl J., Čapek J., Majtnerová P., Báčová J., Roušar T. The effect of repeated passaging on the susceptibility of human proximal tubular HK-2 cells to toxic compounds. *Physiological Research,* 2020, 69, *ISSN 0862-8408, https://doi.org/10.33549/physiolres.934491*. ***(IF = 1,701)***

Motola M., Čapek, J., Zazpe, R., Báčová, J., Hromádko, L. - Brůčková, L., Ng, S., Handl, J., Spotz, Z., Knotek, P., Baishya, K., Majtnerová, P., Přikryl, J., Sopha, H., Roušar, T., Macák, J. Thin TiO_2 Coatings by ALD Enhance the Cell Growth on TiO_2 Nanotubular and Flat Substrates. *ACS Applied BioMaterials,* 2020, 3 (9), 6447-6456. *ISSN: 2576-6422, https://doi.org/10.1021/acsabm.0c00871*. **(*Will be determined)***

Handl J., Čapek J., Majtnerová P., Petira F., Hauschke M., Roušarová E., Roušar T. Transient increase in cellular dehydrogenase activity after cadmium treatment precedes enhanced production of reactive oxygen species in human proximal tubular kidney cells. *Physiological Research*, 2019; 68:481-490. *ISSN 0862-8408, https://doi.org/10.33549/physiolres.934121. (**IF = 1,701**)*

International conferences – Posters

Majtnerová P., Pryszcz L., Heidingsfeld O. Useful tools for differentiation and quantification of the yeast species *Candida albicans* and *Candida guillermondii* in mixed samples. 44th ANNUAL CONFERENCE ON YEAST, Smolenice, Slovensko, **2.5.-5.5.2017**.

Bacova J., Majtnerova P., Hromadko L., Macak J. M., Rousar T.: Assessment of potential toxicity of new synthesized nanofibers in pulmonary cells *in vitro*. EUROTOX 2019, Helsinky, Finsko, **8.-11.9.2019,** Toxicology Letters 314 (S1), str. 209 (2019), *ISSN 0378-4274*.

Čapek J., Brychtová V., Handl J., Majtnerová P., Roušar T. Characterization of cadmium induced apoptosis. TOXCON 2018: 23rd Interdisciplinary Toxicology Conference, Stará Lesná, **20.-22.6., 2018**.

Handl J., Čapek J., Majtnerová P., Roušar T.: Estimation of redox status in kidney cells treated with cadmium. TOXCON 2018, Stará Lesná, Slovakia, **20.-22.6.2018**.

The financial support was received from the Ministry of Education, Youth and Sports of the Czech Republic via project NANOBIO (Reg. No. CZ.02.1.01/0.0/0.0/17_048/0007421).